Project no. 282688

ECLIPSE

Evaluating the **Cl**imate and Air Quality **I**m**p**acts of **S**hort-Liv**e**d Pollutants

Collaborative Project

Work programme: Climate forcing of non UnFCCC gases, aerosols and black carbon

Activity code: ENV.2011.1.1.2-2

Coordinator: Andreas Stohl, NILU - Norsk institutt for luftforskning

Start date of project: November 1st, 2011

Duration: 36 months

Deliverable D6.5 Assessment of GWP/GTP metrics

Due date of deliverable: project month 36

Actual submission date: project month 40

Organisation name of lead contractor for this deliverable: UREAD

Scientist responsible for this deliverable: Keith P Shine, UREAD

Revision Draft 1

Project co-funded by the European Commission within the Seventh Framework Programme (2007-2013)		
Dissemination Level		
PU	Public	
PP	Restricted to other programme participants (including the Commission Services)	X
RE	Restricted to a group specified by the consortium (including the Commission Services)	
CO	Confidential, only for members of the consortium (including the Commission Services)	

The attached draft paper addresses the issue of the extent to which climate model experiments support the newly proposed Global Precipitation Potential metric discussed in ECLIPSE Deliverable 5.6

It examines the underlying assumption that the fast precipitation response, in this case for ozone, is proportional to the atmospheric effective radiative forcing, and shows, to a good approximation, that it is. It also shows clearly that, in the climate model, the precipitation response to tropospheric ozone increases and stratospheric ozone depletion are opposite in sign.

Contrasting precipitation response to tropospheric and stratospheric ozone forcing

C. R. Macintosh, L. H. Baker, N. Bellouin, W. Collins and K. P. Shine*

Department of Meteorology, University of Reading, Reading RG6 6BB, UK

*Corresponding author

To be submitted as a Letter to either *Nature Climate Change* or *Nature Geoscience*

Human activity has caused tropospheric and stratospheric ozone concentrations to change. Ozone change contributes to surface temperature change (Myhre et al. 2013) by perturbing top-of-atmosphere radiative fluxes (radiative forcing). The surface-atmosphere partitioning of radiative forcing strongly influences the so-called fast precipitation response (which acts in addition to a slow response that is proportional to surface temperature change). We present the first detailed climate model study of the link between ozone and fast precipitation response and show that the response is highly dependent on the altitude at which ozone changes. Ozone increases in the lower troposphere cause a negative fast precipitation response, while increases at altitudes above about 3 km cause a positive response. Notably, we find that the fast response to stratospheric ozone change is, per unit forcing, about 3 times higher than that due to tropospheric changes. Our results indicate that tropospheric ozone increases over recent decades will have overall caused a negative fast precipitation response. By contrast, stratospheric ozone depletion over the same period will have caused a positive response. As the relative importance of tropospheric and stratospheric ozone forcing is expected to change in the future, so too will the net impact of ozone change on precipitation.

Recent research (e.g. Allen and Ingram (2002), Allan et al. (2014), Andrews et al. (2010), Thorpe and Andrews (2014)) has led to a theoretical framework, based on energetic constraints, for understanding the global precipitation response to climate perturbations. A simple model of the relationship between top-of-atmosphere radiative forcing (RF), surface temperature change (ΔT) and global-mean precipitation change (ΔP), can be written by separating the precipitation response into a so-called "slow response", related to the surface temperature change, and a fast response, dependent on the partitioning of the RF between the surface and atmosphere, such that

$$L\Delta P \approx k\Delta T - fRF \qquad (1)$$

where L is the latent heat of vaporisation and k and f are constants, which are model dependent and f is also dependent on the forcing agent. Physically, this relationship arises because the global-mean tropospheric energy budget can be viewed, to first order, as a net radiative cooling balanced by latent heating due to condensation of water vapour. In steady state, the rate of condensation is identical to the global-mean evaporative flux and hence precipitation. f is the fraction of the RF felt by the atmosphere (i.e. $fRF = RF_{atm}$).The last term in Eq. (1) is therefore the change in the tropospheric radiative budget due to the fraction of RF which is felt directly by the atmosphere (as opposed to the surface); the first right-hand

side term is due to subsequent warming and moistening of the atmosphere resulting from ΔT. The parameter *k* can be derived from climate model simulations and can include the effect of changes in surface sensible heat fluxes on the tropospheric energy budget (Lambert and Webb 2008, Andrews et al. 2010). We use two forms of RF (Myhre et al. 2013) depending on the particular purpose. The more traditional RF computes the change in net irradiances at the tropopause, assuming surface temperature and tropospheric conditions (temperature, humidity, cloudiness, etc) remain fixed, but stratospheric temperature responds to maintain global-mean radiative equilibrium. The effective radiative forcing (ERF) assumes only surface temperature to remain fixed, but allows tropospheric conditions to adjust. Surface temperature response is more directly related to ERF, but its calculation is more involved and the traditional RF remains a useful metric for many purposes.

Climate model simulations (Andrews et al. 2010; Kvalevåg et al. 2013) have found that *f* is highly dependent on the species under consideration. For CO_2, *f* is found to be positive, so that the fast response acts to oppose the slow response. Andrews et al. (2010) found that *f* for ozone changes was negative (-0.3) and so acts to enhance the slow response. Using the current best estimate of historical ERF due to tropospheric ozone (Myhre et al. 2013), the equilibrium precipitation response, using Andrews et al's *f* factors, would be about 35% that of CO_2; this is disproportionally strong compared to tropospheric ozone ERF (and hence the equilibrium ΔT), which is only 20% that of CO_2.

Ozone therefore appears to have a sizeable influence on precipitation. Unfortunately, previous studies did not distinguish stratospheric and tropospheric ozone perturbations and could not explain their combined responses. We provide a robust theoretical framework for understanding the factors that drive the total precipitation response to ozone change. We first use RF calculations to show the dependence of RF_{atm} on the altitude of the ozone perturbation. We then use a sophisticated atmospheric general circulation model (GCM) to compute the fast precipitation response for both idealised and more-realistic ozone perturbations.

If the thermal infrared component of RF is taken to be the most-height dependent component of the forcing (as will be shown below), then a simple conceptual model can be used to anticipate the response. The net effect of an ozone increase depends on the compensation between the increase in the amount of surface-emitted radiation absorbed by the atmosphere (which leads to a positive RF_{atm}) and the increased atmospheric emission of radiation (which leads to a negative RF_{atm}). In the warm lower troposphere, the emission term is typically the largest, while in the colder upper troposphere, the absorption term is more important. A simple grey-body model can be used to illustrate that the net RF_{atm} is likely to change sign in the mid-troposphere. Such a change in sign (at around 700 hPa) has previously been shown, using detailed calculations, in response to increased water vapour (Previdi, 2011).

We quantify the effect for ozone by conducting a set of idealised perturbation experiments using an offline radiation code applied to realistic present-day zonal-mean ozone concentrations (see *Methods)* which are increased by 20% in each atmospheric layer in turn. RF, RF_{atm} and *f* are calculated for both cloud-free and all-sky (i.e. cloud-free and cloudy) cases (Figure 1). Stratospheric ozone change influences RF_{atm} mostly via the induced change in stratospheric temperature (e.g. Ramaswamy et al. 1992), which then influences downwelling thermal infrared radiation at the tropopause.

Figure 1a shows the very strong dependence of RF_{atm} on the height of the ozone perturbation, with only a small dependence on whether clouds are present. At pressures above about 600 hPa, RF_{atm} is negative, and so from Equation (1), the fast component of the precipitation response is expected to be positive for an ozone increase. Figure 1a and 1b show that this behaviour is largely driven by thermal infrared processes. Nevertheless, the shortwave perturbation significantly modifies both the pressure at which RF_{atm} changes sign and the magnitude of RF_{atm} in the upper troposphere and lower stratosphere. For comparison, RF itself (Figure 1c) is also dependent on the height of the ozone perturbation, as shown by Lacis et al. (1990) and Forster and Shine (1997), but it remains positive throughout the troposphere and lower stratosphere; it only becomes negative in the upper stratosphere (Lacis et al., 1990) above the region of interest here. These new results highlight the crucial dependence of *f* on the vertical distribution of ozone change (Figure 1d). Because the surface temperature response, driven by RF, is positive for an ozone increase, the associated fast response of precipitation will enhance the slow response in the lower troposphere but oppose it at higher altitudes.

Since the link between RF and precipitation change discussed above is based on a simple model (Equation 1), it is important to test it within a model that explicitly simulates precipitation processes and their interaction with radiation, and which enables the ERF to be derived. We use the Met Office Hadley Centre atmosphere model HadGEM3 (see *Methods*) to investigate the fast precipitation response for a number of idealised and more realistic ozone perturbations. We present evidence of a significant influence of ozone change on clouds (a so-called semi-direct effect), which contributes to the difference between RF and ERF, in the Supplementary Information.

Four idealised scenarios are constructed. The first, lower troposphere (LT), perturbs ozone from the surface to 700 hPa. The second, upper troposphere (UT), perturbs the remainder of the troposphere. The third is a combination of these (LT+UT) and tests the additivity of UT and LT. The fourth (ST) decreases stratospheric ozone. A vertically-uniform perturbation of present-day ozone mixing ratios of 100% is applied for the LT, UT and LT+UT, and a 20% reduction is applied for ST. Table 1 shows the global-mean results for these experiments for ERF, ERF_{atm}, and the resulting *f* (i.e., ERF_{atm}/ERF). The validity of the simple model of the fast response (Equation 1) is assessed by comparing the predicted response (from minus ERF_{atm}) with the GCM-calculated change in precipitation (multiplied by *L* to convert to W m^{-2}).

Table 1 shows that LT leads to a global precipitation increase in the GCM whereas UT leads to a decrease, despite the fact that the ERF is positive for both cases. The ST experiment leads to a precipitation increase; because this is in response to a decrease in ozone, the sense of the response (i.e. an ozone increase leads to a precipitation decrease) is the same for UT and ST. ERF_{atm} predicts this behaviour well, confirming the utility of the simple conceptual model; quantitatively the precipitation change predicted using ERF_{atm} is within about 25% of the GCM response. The sign difference between the LT and UT precipitation response is as anticipated from Figure 1, showing that the physical reason for this behaviour is understood. LT+UT is within 5% of the sum of the individual LT and UT cases, and shows that the UT perturbation dominates the precipitation response. There is substantial variation in *f* with height; it is largest for stratospheric perturbations, and positive in all cases except LT.

Stratospheric ozone changes are, per unit ERF, roughly 4 times more effective in influencing the fast precipitation response than LT+UT changes.

Having clarified the driving mechanisms, calculations with more realistic ozone changes are performed to understand the role of ozone changes in the present-day climate. We impose ozone changes between the pre-industrial and the present-day (2000) atmosphere, using multi-model means from the Atmospheric Chemistry and Climate Model Intercomparison Project (ACCMIP) (Young et al. 2013) (see *Methods*), for the troposphere only, the stratosphere only, and both together. Table 1 show that, overall, changes to tropospheric ozone act to decrease precipitation; this means that for actual changes in ozone, as well as the idealised ones used for LT and UT, upper tropospheric changes are more influential than lower troposphere changes. Stratospheric ozone depletion leads to an increase in precipitation and, as was found for the idealised experiments, the value of f is much larger (by about a factor of 3 for this case) than that for tropospheric ozone changes. As with the idealised experiments, the full (stratosphere plus troposphere) response is found to be sum of the individual components to a good approximation. The resulting full atmospheric ERF is positive, but very small, and the overall f is close to zero showing the net effect of the stratospheric and tropospheric ozone changes on the fast precipitation response almost cancel in present-day conditions, despite the tropospheric ozone ERF being 3.5 times the stratospheric ozone ERF. By contrast, Andrews et al. (2010) find a net ozone ERF of 0.16 W m^{-2} for the pre-industrial to 1990 period, and an f of -0.3, indicating that, in their calculation, stratospheric ozone depletion is more influential.

These results strongly support the primary role of the atmospheric energy constraint in driving the effect of ozone on the fast component of global-mean precipitation change encapsulated in Equation (1). Across all the GCM experiments presented in Table 1, there is a very strong correlation (r^2 in excess of 0.99) between ERF_{atm} and precipitation change. The study has, for the first time, demonstrated the effectiveness of stratospheric ozone change in driving this fast component.

The drivers of tropospheric ozone change are mostly emissions of short-lived pollutants, which influence surface air quality (e.g. methane, oxides of nitrogen, carbon monoxide and volatile organic compounds) while stratospheric ozone change is driven mostly by emission of much longer-lived halocarbons. The emissions of these drivers has changed markedly in the past; for example, during the 1950s the magnitude of the ERF from tropospheric ozone is estimated to be have been a factor of at least 25 times greater than that due to stratospheric ozone, compared to a 2011 value of about 8 (Myhre et al. (2013)). Although much more uncertain, the relative importance seems likely to change markedly again in the future. Our work shows how important it is to quantify separately the effect of tropospheric and stratospheric ozone changes on precipitation. This is especially the case when GCM output is used in simple model approaches (such as Thorpe and Andrews (2014)), which exploit the simple conceptual approach in Equation (1).

Methods

Radiative forcing calculations shown in Figure 1 are derived using the offline Edwards-Slingo (1996) radiation code with 9 longwave and 6 shortwave spectral bands. Incoming solar radiation at mid-month and a 6-point Gaussian integration over daylight hours is used to calculate the day-averaged shortwave forcing. The calculations are performed on a 2.5^o x 3.75^o horizontal grid at 22 levels, using temperatures and humidity profiles from European Centre for Medium-range Weather Forecasts reanalysis (Uppala et al., 2005) with cloud amount and surface albedos from the International Satellite Cloud Climatology Project (Rossow and Schiffer, 1999). The ACCMIP multi-model-mean present-day ozone zonal-mean distribution (minus those from the MOCAGE model in the stratosphere) (Young et al. 2013) is perturbed by increasing ozone by 20% in each atmospheric layer in turn. Stratospheric temperature adjustment is applied using the fixed-dynamical heating method, with the tropopause defined as the level at which the lapse rate falls below 2 K km^{-1}. Annual-mean values are derived as means from January, April, July and September.

The HadGEM3 climate model is used with an atmospheric resolution of 1.875° x 1.25° and 63 vertical levels between the surface and 40 km (Hewitt et al. 2011). It uses the Edwards and Slingo (1996) radiation scheme. Simulations are for 3–year long (2008-2010) with sea surface temperatures and sea ice from the AMIP climatology. In order to reduce the variability in cloud distributions between the different simulations, model winds above the boundary layer are nudged towards ERA-Interim analyses following Telford et al. (2008). Ozone fields were imposed as monthly-varying zonal-mean climatologies.

For the idealised scenarios a control simulation was run with the year 2000 ozone climatology. Subsequent simulations were made by doubling the ozone mixing ratios between the surface and 700 hPa (LT), 700 hPa and the tropopause, and between the surface and the tropopause (LT+UT). The ST perturbation was a 20% decrease in ozone mixing ratios between the tropopause and the model top (40 km). The 150 nmol mol^{-1} ozone contour was used to identify the tropopause for this purpose. The differences in the top-of-atmosphere longwave and shortwave fluxes between the control and each perturbation simulation give the ERFs. Similarly the differences in the surface longwave and shortwave fluxes give the effective surface forcing (ERF_{surf}). The atmospheric effective forcing (ERF_{atm}) is then given by ERF-$ERF_{surf.}$

For the realistic scenarios the control simulation uses the 1850 ACCMIP ozone climatology (Young et al. 2013). To amplify the signal, tropospheric ozone is perturbed by twice its historical change below the tropopause, i.e DeltaTropOzone = 2×(2000-1850)+1850. The values for "Full Troposphere" in Table 1 have been divided by 2. The "stratosphere" perturbation used year 2000 ozone mixing ratios above the tropopause, and the "Full atmosphere" perturbation used year 2000 ozone mixing ratios throughout the atmosphere.

References (no more than 30)

1. Allan, R. P., C. L. Liu, M. Zahn, D. A. Lavers, E. Koukouvagias, and A. Bodas-Salcedo. 2014. Physically Consistent Responses of the Global Atmospheric Hydrological Cycle in Models and Observations. *Surveys in Geophysics* 35 (3):533-552.
2. Allen, M. R., and W. J. Ingram. 2002. Constraints on future changes in climate and the hydrologic cycle. *Nature* 419 (6903):224-232.
3. Andrews, T., P. M. Forster, O. Boucher, N. Bellouin, and A. Jones. 2010. Precipitation, radiative forcing and global temperature change. *Geophysical Research*

Letters 37.
4. Edwards, J. M., and A. Slingo. 1996. Studies with a flexible new radiation code .1. Choosing a configuration for a large-scale model. *Quarterly Journal of the Royal Meteorological Society* 122 (531):689-719.
5. Forster, PMD, and KP Shine. 1997. Radiative forcing and temperature trends from stratospheric ozone changes. *Journal of Geophysical Research-Atmospheres* 102 (D9):10841-10855.
6. IPCC. 2013. *Climate Change 2013: The Physical Science Basis. Contribution of Working Group I to the Fifth Assessment Report of the Intergovernmental Panel on Climate Change*. Cambridge, United Kingdom and New York, NY, USA: Cambridge University Press.
7. Kvalevag, M. M., B. H. Samset, and G. Myhre. 2013. Hydrological sensitivity to greenhouse gases and aerosols in a global climate model. *Geophysical Research Letters* 40 (7).
8. Hewitt, H.T, D. Copsey, I. D. Culverwell, C. M. Harris, R. S. R. Hill, A. B. Keen, A. J. McLaren, and E. C. Hunke. 2011 Design and implementation of the infrastructure of HadGEM3: the next-generation Met Office climate modelling system. *Geosci. Model Dev*., 4, 223–253
9. Lacis, A. A., D. J. Wuebbles, and J. A. Logan. 1990. Radiative forcing of climate by changes in the vertical-distribution of ozone. *Journal of Geophysical Research-Atmospheres* 95 (D7):9971-9981.
10. Lambert, F. H., and M. J. Webb. 2008. Dependency of global mean precipitation on surface temperature. *Geophysical Research Letters* 35 (16).
11. Myhre, G., D. Shindell, F.-M. Bréon, W. Collins, J. Fuglestvedt, J. Huang, D. Koch, J.-F. Lamarque, D. Lee, B. Mendoza, T. Nakajima, A. Robock, G. Stephens, T. Takemura, and H. Zhang. 2013. Anthropogenic and Natural Radiative Forcing. In *Climate Change 2013: The Physical Science Basis. Contribution of Working Group I to the Fifth Assessment Report of the Intergovernmental Panel on Climate Change*, edited by T. F. Stocker, D. Qin, G. K. Plattner, M. Tignor, S. K. Allen, J. Boschung, A. Nauels, Y. Xia, V. Bex and P. M. Midgley. Cambridge, United Kingdom and New York, NY, USA: Cambridge University Press.
12. Previdi, M. 2010. Radiative feedbacks on global precipitation. *Environmental Research Letters* 5 (2).
13. Ramaswamy, V, MD Schwarzkopf, and KP Shine. 1992. Radiative forcing of climate from halocarbon-induced global stratospheric ozone loss. *Nature* 355 (6363):810-812.
14. Rossow, W. B., and R. A. Schiffer. 1999. Advances in understanding clouds from ISCCP. *Bulletin of the American Meteorological Society* 80 (11):2261-2287.
15. Telford, P.J., P. Braesicke, O. Morgenstern, and J. A. Pyle. 2008. Technical Note: Description and assessment of a nudged version of the new dynamics Unified Model. *Atmos. Chem. Phys*., 8, 1701-1712.
16. Thorpe, L., and T. Andrews. 2014. The physical drivers of historical and 21st century global precipitation changes. *Environmental Research Letters* 9 (6).
17. Uppala, S. M., P. W. Kallberg, A. J. Simmons, U. Andrae, V. D. Bechtold, M. Fiorino, J. K. Gibson, J. Haseler, A. Hernandez, G. A. Kelly, X. Li, K. Onogi, S. Saarinen, N. Sokka, R. P. Allan, E. Andersson, K. Arpe, M. A. Balmaseda, A. C. M. Beljaars, L. Van De Berg, J. Bidlot, N. Bormann, S. Caires, F. Chevallier, A. Dethof, M. Dragosavac, M. Fisher, M. Fuentes, S. Hagemann, E. Holm, B. J. Hoskins, L. Isaksen, Paem Janssen, R. Jenne, A. P. McNally, J. F. Mahfouf, J. J. Morcrette, N. A. Rayner, R. W. Saunders, P. Simon, A. Sterl, K. E. Trenberth, A. Untch, D. Vasiljevic, P. Viterbo, and J. Woollen. 2005. The ERA-40 re-analysis. *Quarterly Journal of the*

Royal Meteorological Society 131 (612):2961-3012.
18. Young, P. J., A. T. Archibald, K. W. Bowman, J. F. Lamarque, V. Naik, D. S. Stevenson, S. Tilmes, A. Voulgarakis, O. Wild, D. Bergmann, P. Cameron-Smith, I. Cionni, W. J. Collins, S. B. Dalsoren, R. M. Doherty, V. Eyring, G. Faluvegi, L. W. Horowitz, B. Josse, Y. H. Lee, I. A. MacKenzie, T. Nagashima, D. A. Plummer, M. Righi, S. T. Rumbold, R. B. Skeie, D. T. Shindell, S. A. Strode, K. Sudo, S. Szopa, and G. Zeng. 2013. Pre-industrial to end 21st century projections of tropospheric ozone from the Atmospheric Chemistry and Climate Model Intercomparison Project (ACCMIP). *Atmospheric Chemistry and Physics* 13 (4):2063-2090.

Acknowledgements

This work was funded by the European Commission, under the ECLIPSE (Evaluating the Climate and Air Quality Impacts of Short-Lived Pollutants) Project (Grant Agreement 282688). We thank other ECLIPSE partners for their input to this work.

Author Contributions

LB, WC, CM and KS conceived the study; CM performed the RF calculations, LB performed the GCM calculations, with all authors contributing to the analysis and interpretation. KS and CM led the writing of the paper with input from LB, NB and WC.

Competing Financial Interests

The authors declare no competing financial interests.

Ozone change	Experiment	ERF (W m^{-2})	ERF_{atm} (W m^{-2})	LΔP (W m^{-2})	f
Idealised	Troposphere + 100%	1.11	0.48	-0.37	0.43
Idealised	Lower Trop +100%	0.28	-0.12	0.10	-0.42
Idealised	Upper Trop +100%	0.83	0.58	-0.46	0.70
Idealised	Stratosphere – 20%	-0.27	-0.46	0.36	1.70
Pre-industrial to present day	Full Atmosphere	0.26	0.006	0.005	0.02
Pre-industrial to present day	Full Troposphere	0.36	0.13	-0.10	0.36
Pre-industrial to present day	Stratosphere	-0.096	-0.12	0.11	1.27

Table 1: Top-of-atmosphere and atmospheric effective radiative forcing, precipitation change multiplied by the latent heat of vapourization (all in W m^{-2}) and f (i.e. ERF_{atm}/ERF) for climate model simulations for 4 idealised ozone perturbations (top rows) and 3 more realistic cases (bottom rows).

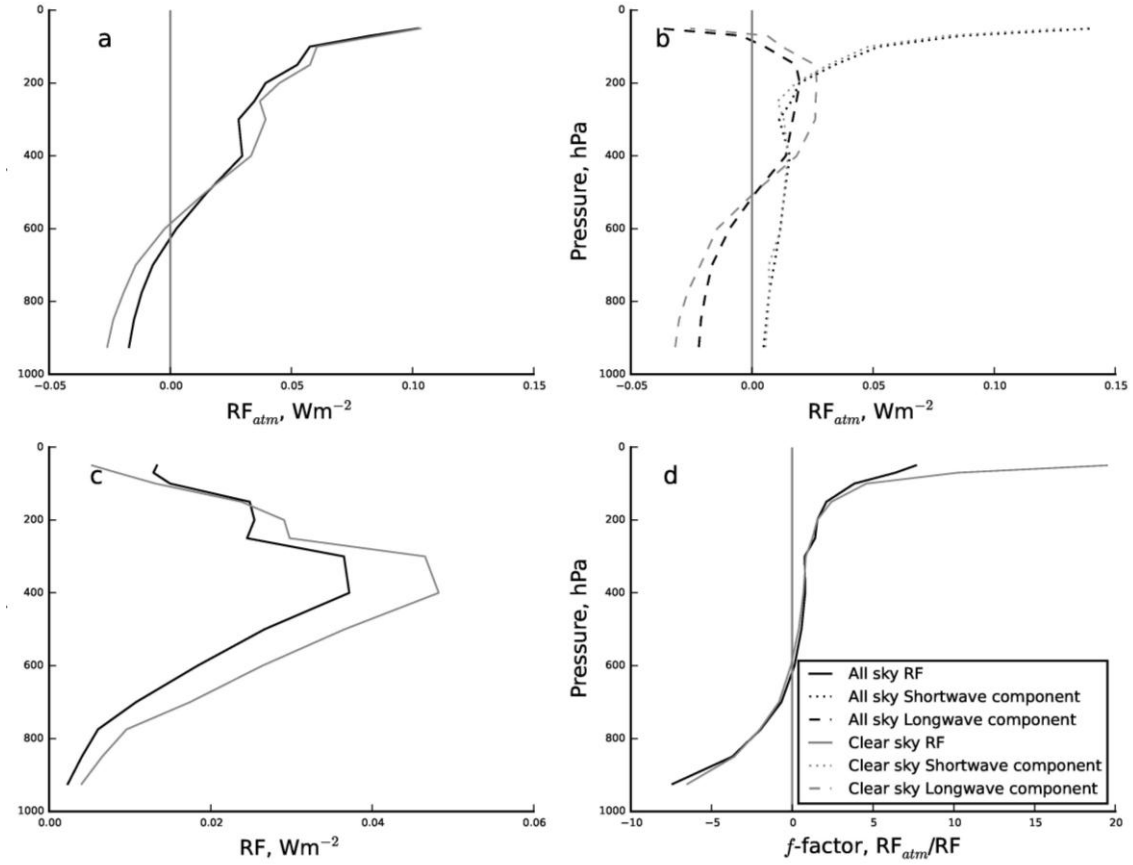

Figure 1: Impact of 20% global increases in ozone applied in each atmospheric layer in turn on RF, RF_{atm} and *f*. The vertical coordinate is the pressure at which the perturbation is applied. a) RF_{atm}; b) longwave (including stratospheric adjustment) and shortwave components of a); c) RF; d) the parameter *f*= RF_{atm}/RF.

Supplementary Information

We briefly discuss the annual- and zonal-mean latitudinal distribution of precipitation changes, and the role of cloud changes in influencing the ERF, for the idealised GCM calculations, LT, UT and ST.

Figure S1 frames (a), (d) and (g) shows the structure of the atmospheric ERF (for clear-sky and all-sky cases). It also shows the change in cloud radiative forcing between the control and perturbed case. Clear and all-sky forcings are expected to differ, because clouds strongly modulate the shortwave and longwave radiation fields, but the GCM results illustrate a marked difference between the clear and all-sky ERFs (shown by the change in cloud forcing), particularly in the LT case (frame (a)), which is larger than could be anticipated from the RF calculations shown in Figure 1. This is indicative of a significant semi-direct cloud response (i.e. a response that is independent of any surface temperature change) to the ozone perturbation, which then contributes to the ERF.

Frames (b), (e) and (h) show the precipitation changes largely occurs in the tropics in all cases, and illustrates further the contrasting response of precipitation to LT and UT/ST changes in ozone.

Frames (c), (f) and (i) show one indicator of cloud response in the model, the change in mid and high cloud fraction, as a result of the ozone perturbations. The response is complex, but for all three simulations a signature related to (and the same size as) changes in tropical precipitation can clearly be seen.

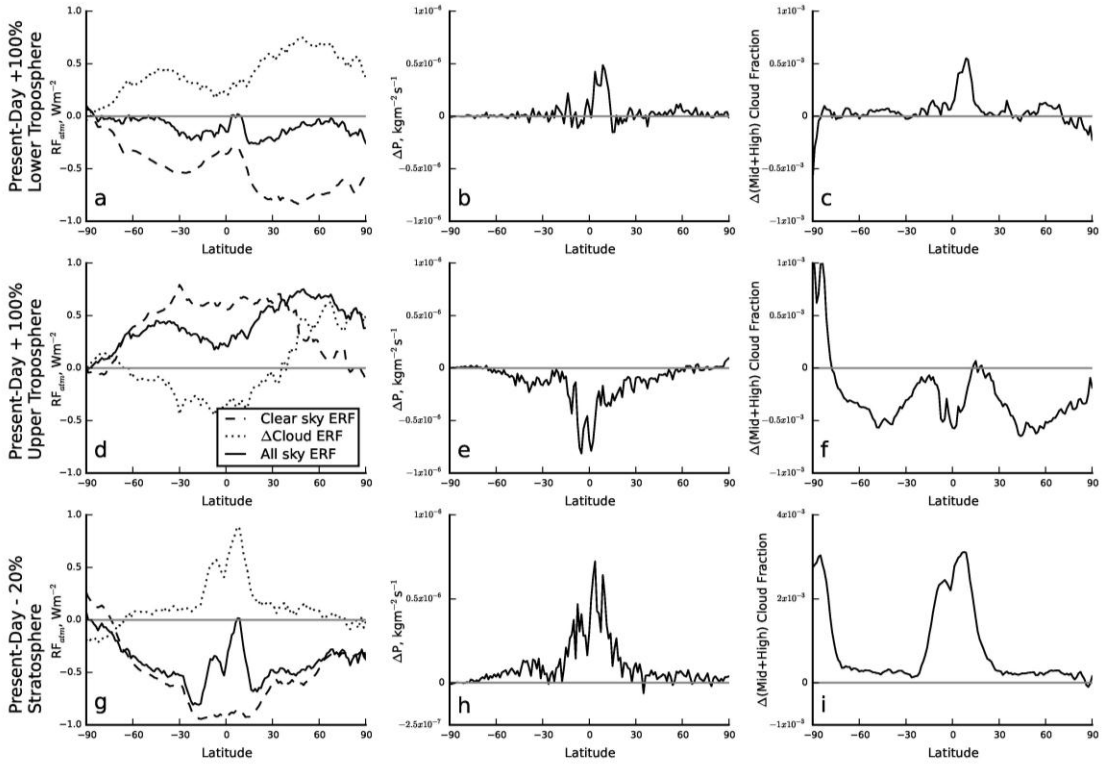

Figure S1: Zonal and annual-mean ERFs (left column), precipitation changes (middle column) and mid plus high cloud changes (right column) for the idealised ozone perturbation GCM simulations. The LT simulations are shown in the top row, the UT (middle row) and ST (bottom row).